Heat and/or mass transfer intensification in helical pipes: Optimal helix geometries and comparison with alternative enhancement techniques

Omran Abushammala, Rainier Hreiz, Cécile Lemaître, Eric Favre

Version of Record: https://www.sciencedirect.com/science/article/pii/S0009250921000178
Manuscript_96c0ff8eb4c5f0df0f12cc96b074434e

Heat and/or Mass transfer intensification in helical pipes: optimal helix geometries and comparison with alternative enhancement techniques

Omran Abushammala[a,b], Rainier Hreiz[a*], Cécile Lemaître[a], Éric Favre[a]

[a]Laboratoire Réactions et Génie des Procédés, Université de Lorraine, CNRS, LRGP, F-54000 Nancy, France.
[b]Eden Tech, 172 rue de Charonne, 75011, Paris, France.
[*]Corresponding author at:
Rainier Hreiz, Laboratoire Réactions et Génie des Procédés, Université de Lorraine, ENSIC, CNRS, LRGP, 1 rue Grandville, 54001 Nancy, France. Tel: +33 (0) 372 743 876; E-mail address: rainier.hreiz@univ-lorraine.fr

Abstract
Maximizing the transfer performances of heat and mass exchangers is a major target for process intensification purposes. Basically, flux enhancement can be achieved through increased specific surface area and/or increased transfer coefficients (e.g. Dean vortices generation in curved pipes), but this has to be balanced to energy requirement. In this study, novel performance criteria taking into account both specific surface area effects and the associated friction losses are proposed and applied to helical pipe exchangers covering a broad range of geometries. It is shown that most helical pipe geometries exhibit poor efficiencies in terms of volumetric transfer rates. Nevertheless, some very particular helix designs are shown to offer a huge potentiality for intensified heat/mass transfer performances. Surprisingly, a major volume reduction is indeed shown to be achievable together with a decreased energy requirement (pumping power). The performances of these novel designs are finally critically compared to alternative process intensification techniques.

Keywords: Heat transfer; Helical pipe; Intensification; Mass transfer; Packing density; Specific surface area

1. Introduction

Active research on heat/mass transfer enhancement is driven by the purpose of reducing both equipment size and energy requirement, i.e. saving material and minimizing operating costs. In particular, compact and lightweight units are of primary interest in applications with mobile operation and/or where space is limited, e.g. transport systems, decentralized energy production, domestic applications, space and offshore processes. In addition, as they contain less fluid, compact systems significantly reduce the risk of thermal runaway as well as the consequences of a process failure (e.g. leakage) if hazardous fluids are used. Moreover, in the case of chemical reactors or multifunctional heat exchangers, enhanced heat and mass transfer rates allow achieving better yields and selectivities.

Various techniques have been investigated in the literature in order to enhance heat/mass transfer between a flowing fluid and the surrounding pipe walls (Winzeler and Belfort, 1993; Liu and Sakr, 2013; Alam and Kim, 2018). They include the use of internals (e.g. twisted tapes, swirl devices, vortex generators), artificial wall roughness, pulsatile flow and/or the use of curved pipe geometries (e.g. helical or coiled designs) which generate Dean-type secondary flows or lead to chaotic advection. Compared to the base case of smooth straight pipes without any inserts and under steady flow conditions (which will be simply referred as 'the base case' further on in this paper), these techniques allow enhancing the convective transfer rate, however, they induce higher frictional losses per unit length. Therefore, in this context, the main challenge when improving existing techniques or designing novel geometries is to simultaneously address these conflicting criteria, i.e. significantly improving the heat/mass transfer while maintaining the pressure drop as low as possible.

Several performance criteria, combining these two conflicting objectives, have been proposed in the literature to evaluate and compare the effectiveness of enhancement strategies. They are generally expressed as follows (for heat and mass transfer situations respectively):

$$\eta_{1,n} = \frac{Nu/Nu_S}{\left(C_f/C_{f,S}\right)^n} \quad or \quad \eta_{1,n} = \frac{Sh/Sh_S}{\left(C_f/C_{f,S}\right)^n} \qquad \text{Eq. 1}$$

Nu, Sh and C_f without subscript receptively designate the effective Nusselt number, Sherwood number and friction coefficient, obtained when the enhancement technique is applied, whereas the subscript S refers to the base case of a smooth straight pipe. Exponent n is a positive weighting factor: a value of 1 indicates that similar importance is accorded to both objectives, while a value lower than unity indicates that a higher priority is given to heat/mass transfer enhancement to the detriment of the friction coefficient increase. η designates the performance evaluation criterion, and subscripts 1 and n respectively refer to the powers of the Nu (or Sh) and C_f ratios.

A frequently used performance index is $\eta_{1,1}$ (Bhadouriya et al., 2015) which is expressed as follows:

$$\eta_{1,1} = \frac{Nu/Nu_S}{C_f/C_{f,S}} \quad or \quad \eta_{1,1} = \frac{Sh/Sh_S}{C_f/C_{f,S}} \qquad \text{Eq. 2}$$

It compares the heat/mass transfer enhancement allowed by a given method or design to the relative friction coefficient increase that it induces. As it attributes similar weights to both factors, $\eta_{1,1}$ can be interpreted as an assessment of the energy-efficiency of the considered enhancement technique.

However, the most widely used performance indicator is $\eta_{1,1/3}$, initially introduced by Webb and Eckert (1972), and which is defined as follows:

$$\eta_{1,1/3} = \frac{Nu/Nu_S}{\left(C_f/C_{f,S}\right)^{1/3}} \quad or \quad \eta_{1,1/3} = \frac{Sh/Sh_S}{\left(C_f/C_{f,S}\right)^{1/3}} \qquad \text{Eq. 3}$$

$\eta_{1,1/3}$ aims at comparing the transfer performance of an enhancement technique/design to that of the base case, under equal pipe length and pumping power conditions, whence the power (1/3) over the friction coefficients ratio. However, in the context of process intensification, the use of the $\eta_{1,1/3}$ index is not always relevant. Indeed, to transfer a given heat/mass flux, enhanced heat/mass exchangers require shorter pipe lengths than the base case. Therefore, since by definition $\eta_{1,1/3}$ assumes equal pipe lengths in both situations, this performance index will not be used in this paper for evaluating and comparing the effectiveness of different augmentation strategies.

A third performance index following the general form presented in Equation 1 is $\eta_{1,0}$, which simply corresponds to the Nusselt numbers (respectively Sherwood numbers) ratio. This evaluation criterion is appropriate in situations where pumping costs are not an issue, for example when the working fluids are available at sufficient pressure.

As can be noticed, evaluation criteria based on the general expression given in Equation 1 assess the transfer efficiency via the *Nu* or *Sh* numbers, i.e. in terms of transfer rate per pipe unit area. Therefore, they are not relevant for characterizing the potential of novel designs in terms of process intensification, i.e. in terms of allowed unit volume reduction. To make things clearer, the example of heat/mass transfer enhancement via the use of helical pipes can be considered. Compared to the base case, these designs are known to lead to a significant improvement of the convective transfer rate for a moderate increase of the pressure drop only. Consequently, helical pipes constitute an efficient enhancement technique according to criteria based on the definition given in Equation 1. Nonetheless, in many heat/mass transfer applications (e.g. hollow fiber membrane contactors, monolith catalytic reactors, shell-and-tube and printed-circuit heat exchangers), a large number of flow tubes is needed. However, helical pipes cannot be as densely packed as straight ones, i.e. cannot occupy the available space as efficiently as straight tubes. Thus, they present a lower specific surface area which can counterbalance the convective transfer enhancement they provide. For example, Kaufhold et al. (2012) reported that when the helix radius is not sufficiently small, helical pipes lead to inferior performance than straight tubes in terms of volumetric transfer rates, i.e. heat/mass flux per unit volume. Thus, since they do not account for packing density effects, evaluation indexes based on the general form given in Equation 1 do not allow assessing the intensification potentiality of novel pipe designs for applications where a large number of tubes are to be packed.

So, the question arises as to whether helically coiled tubes are advantageous in terms of process intensification for heat/mass transfer applications. Can they compete with alternative heat/mass transfer intensification techniques? In an attempt to answer these questions, improved evaluation criteria, accounting for specific surface area effects, are presented in this paper. Based on previously developed correlations for determining the heat/mass transfer coefficient, friction coefficient and packing density, the performances of helical pipes under laminar flow operation are analyzed. Comparison is carried out with available literature studies that investigated the effectiveness of different inserts, pulsatile flow conditions and novel pipe designs. The results reveal that most helical pipe geometries exhibit poor efficiencies in terms of volumetric transfer rates. Nonetheless, some particular helix designs, with elongated shapes and/or small helix radiuses, are shown to offer huge potentiality for intensified mass and/or heat transfer performances. These geometries, which can be manufactured by 3D-printing, should allow conceiving cost-effective compact units as they simultaneously enable to decrease the required pumping power and considerably reduce the volume of reactors, heat exchangers and membrane contactors.

2. Transport phenomena in helical pipe flow

Given their high surface-to-volume ratio, fine tubes are desirable for process intensification and are commonly used in many applications such as hollow fiber membranes, monolith catalytic reactors, micro- and

milli-structured heat exchangers. However, turbulent flows which are ordinarily used to improve transfer rates at macro scales are impractical to achieve in miniaturized devices where viscous forces dominate. Therefore, fine tubes are generally operated under laminar flow conditions where lateral mixing, i.e. radial heat/mass transfer, occurs under the sole effect of conduction/diffusion, which leads to lower convective transfer rates than turbulent flows.

Accordingly, to sustain the full potential of miniaturization, heat/mass transfer enhancement under laminar flow regimes becomes necessary. One possibility to achieve this goal is through the use of helical pipes instead of straight ones. Indeed, the hydrodynamics in helical - and curved - tubes is characterized by the occurrence of a secondary flow consisting of a pair of counter-rotating vortices in the cross-stream direction (i.e. perpendicularly to the primary flow), known as Dean cells (Figure 1a) (Dean, 1927, 1928). These structures provide an efficient advective transport of fluid particles between the pipe walls and its centerline (Figure 1b), leading to increased transfer performance compared to the straight pipes case.

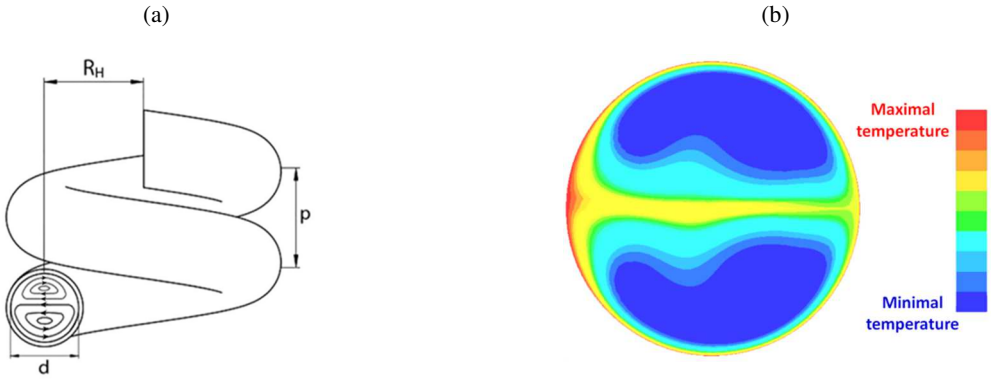

Figure 1: Transport phenomena in helical pipe flows: (a) Schematic representation of Dean cells. (b) Typical fluid temperature field in a cross-section of a heated helical pipe.

Therefore, helical pipes offer attractive potentialities for process intensification and heat/mass transfer enhancement. However, as discussed in the following paragraphs, their performances are very sensitive to their design, flow conditions and to the used working fluid.

2.1. Helical pipes design, packing density and specific surface area

The shape of a helical pipe is described by two geometric parameters, its dimensionless pitch, $p^* = p/d$, and dimensionless helix radius, $R_H^* = R_H/d$, where d is the pipe diameter, p the helix pitch and R_H the helix radius (Figure 1a). Figure 2 illustrates some representative helix designs and the limit of the so-called forbidden region. The equation of this frontier has been determined by Przybył and Pierański (2001): it corresponds to the limit under which it is not possible to further decrease the helix pitch because consecutive turns of the helix would overlap one with another. Thus, the forbidden region corresponds to the set of p^* and R_H^* values for which it is not possible to design helical shapes.

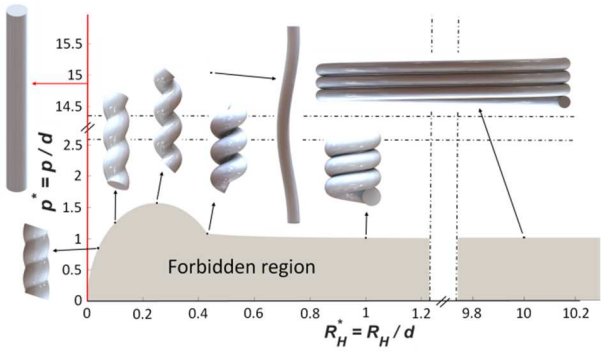

Figure 2: Limit of the forbidden region in the (R_H^* , p^*) space (adapted from Przybył and Pierański (2001)) and some representative helix geometries (Abushammala et al., 2020).

Figure 3 is a contour plot of the dimensionless helix curvature, $\kappa^* = \kappa\, d = d/\gamma$, in the ($R_H^*$, p^*) space, where κ is the helix curvature and γ its curvature radius. The mathematical expression of κ is as follows:

$$\kappa = \frac{1}{R_H\left[1+\left(\frac{p}{2\pi R_H}\right)^2\right]} \qquad \text{Eq. 4}$$

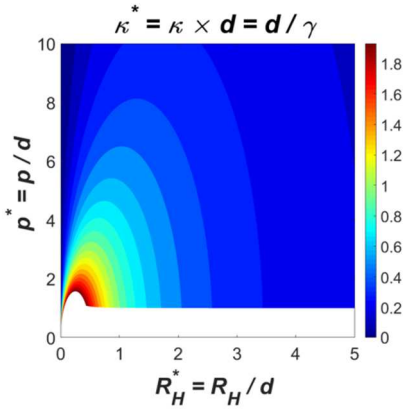

Figure 3: Contour plot of the dimensionless helix curvature, κ^*, in the (R_H^* , p^*) space.

As can be noticed from Figures 2 and 3, helical pipes curvature vanishes when R_H^* tends to zero or when p^* goes to infinity, as the helix shape tends toward that of a cylinder. Thus, at these limits, helical pipes present the same packing density and transfer performances as straight tubes. Furthermore, as R_H^* tends to infinity, helixes curvature vanishes and their shape locally straightens. Thus, at this limit, helical pipes perform as straight tubes from both hydrodynamics and heat/mass transfer point of views, but obviously, they present much lower packing densities than straight pipes.

Most importantly, Figure 3 reveals that the highest curvatures (i.e. lowest radiuses of curvature) are achieved by helixes of low pitch and relatively low helical radius. These geometries have been referred to as Highly Curved Helical Pipes, HCHPs, and it is only recently that their performances in terms of hydrodynamics and heat/mass transfer enhancement were investigated (Abushammala et al., 2019a, 2020). This is probably due to the fact that HCHPs are difficult to manufacture using traditional manufacturing techniques. However, nowadays, thanks to a witnessed progress in 3D-printing, the fabrication of such designs has become achievable. Given their low radius of curvature, HCHPs exhibit high centrifugal effects and produce intense Dean vortices. Thus, as it will be discussed in Section 2.2, they lead to much higher heat/mass transfer rates than 'classical' helical pipes or straight tubes.

As argued earlier, although curved and helical pipe geometries lead to better transfer efficiencies than straight tubes, they cannot be as densely packed, i.e. they present a lower specific surface area. This factor should be necessarily taken into account when quantifying the potential of any new design in terms of process intensification. In fact, it should be checked that the convective heat/mass transfer enhancement it provides is not entirely counterbalanced by its lower specific surface area.

Using a CAD (computer-aided design) software, Abushammala et al. (2020) determined, a_{min}, the minimal achievable distance between non-overlapping helixes disposed in a triangular arrangement (Figure 4a). The study was conducted for different helix geometries and the results allowed calculating, $a_{min}^* = a_{min}/d$, the dimensionless distance separating closely packed helixes, and a correlation (reported in Appendix A) was developed for determining a_{min}^* depending on the helix design, i.e. its $p^*$and R_H^* values. The provided correlation is valid for $p^* \leq 20$ and $R_H^* \leq 10$, although it has been shown to produce reliable results also beyond this range of geometric parameters. It should be noted that a_{min}^* equals unity (i.e. $a_{min} = d$) in the case of straight pipes as can be noticed from Figure 4b.

Figure 4: Top view of: (a) ideally packed helixes of R_H^* = 2.5 and $p^* = 1.25$; (b) ideally packed cylinders. The triangular lattice is illustrated by dashed lines and the black dots represent the axes of the helical or straight tubes.

Figure 5a displays the contour plot of a_{min}^* in the (R_H^* , p^*) space, which was calculated using the correlation of Abushammala et al. (2020). The discontinuity appearing in the contour is due to the fact that different mathematical expressions were used to correlate a_{min}^*, depending on whether R_H^* is lower or higher than 2. As shown by Figure 5a, the lowest possible value for a_{min}^* is 1, and it is achieved when R_H^* is zero or when p^* goes to infinity, i.e. when the helix design approaches that of cylinder (Figure 2). a_{min}^* obviously increases when R_H^* is increased. When p^* increases, the spacing between two consecutive helix turns enlarges. Hence, the different helixes can be brought closer and imbricate, which leads to a decrease of a_{min}^*.

For any helix design, once a_{min}^* is known, its maximum packing density, $\phi_{H,max}$, (which is achieved when the helixes are separated by a distance a_{min}^*) can be easily calculated (Abushammala et al., 2020) and compared to $\phi_{S,max}$, the maximum packing density of cylinders, which equals $\pi/[4\ \sin(\pi/3)] \approx 90.7\%$. The maximal specific surface area (i.e. exchange surface per unit volume) of the set of packed helical pipes, $\sigma_{H,max}$, can be determined relatively to $\sigma_{S,max}$ (the specific surface area of densely packed straight tubes), using the following equation:

$$\frac{\sigma_{H,max}^* \times d_H}{\sigma_{S,max}^* \times d_S} = \frac{\sigma_{H,max}}{\sigma_{S,max}} = \frac{\phi_{H,max} \times s_H}{\phi_{S,max} \times s_S} = \frac{\phi_{H,max} \times 4/d_H}{\phi_{S,max} \times 4/d_S} \qquad \text{Eq. 5}$$

where d denotes the pipe diameter, s the surface-to-volume ratio of a single helical or straight pipe, ϕ_{max} the maximal packing density, σ_{max} the maximal specific surface area and σ_{max}^* its dimensionless form. Subscripts H and S respectively refer to helical and straight pipes. Thus, considering helical and straight pipes having a same diameter, the ratio of their specific surface area equals their packing density ratio. It is noteworthy that Equation 5 also applies to pipe designs other than helical, as long as they present a uniform and circular cross-section.

Figure 5b, adapted from Abushammala et al. (2020), displays the contour plot of the $\sigma_{H,max}^*$ to $\sigma_{S,max}^*$ ratio, which is always lower than unity as helixes cannot be as efficiently packed as straight tubes. Figure 5b reveals that only HCHPs and elongated helical designs (i.e. having a large p^* to R_H^* ratio) present satisfactory specific surface areas (i.e $\sigma_{H,max}^*$ to $\sigma_{S,max}^*$ ratio close to one). Therefore, HCHPs, which also allow a significant convective transfer enhancement (Section 2.2), may be expected to offer huge potentialities for intensified heat/mass transfer performance. On the other hand, 'classical' helixes exhibit very poor packing densities as they cannot efficiently occupy an available space. Therefore, as shown later, these geometries lead to lower performance than straight tubes in terms of volumetric transfer rates.

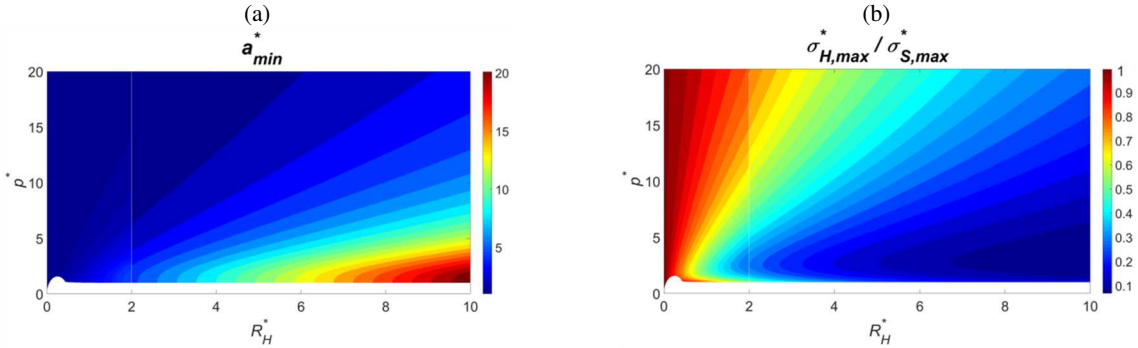

Figure 5: Contour plots in the (R_H^* , p^*) space of (a) a_{min}^* and (b) the $\sigma_{H,max}^*$ to $\sigma_{S,max}^*$ ratio, as calculated using the correlation of Abushammala et al. (2020).

2.2. Hydrodynamics and heat/mass transfer in helical pipe flows

Although heat/mass transfer enhancement using helical pipes has been widely investigated, as reported in Abushammala et al. (2020), literature studies have only dealt with 'classical helixes' with large R_H^* values, probably because these geometries are easy to fabricate using traditional manufacturing techniques. It is only recently that the heat transfer performance of HCHPs was addressed by Abushammala et al. (2020, 2019b) using CFD (computational fluid dynamics). These studies have been conducted under the assumptions of uniform wall temperature and negligible heat generation by viscous dissipation. As discussed in their papers, owing to the heat/mass transfer analogy, their results may be transposed and applied to mass transfer situations in the case of a dilute mixture under uniform wall concentration and in the absence of any homogenous chemical reaction.

Despite that the ideal boundary condition of uniform wall temperature/concentration is rarely met in practice, the results obtained in these papers may be expected to still provide a sufficiently accurate description of transport phenomena in practical situations, as long as the remaining modeling assumptions remain respected.

Furthermore, Abushammala et al. (2020) developed a correlation to predict the fully developed circumference-averaged Nusselt number (respectively Sherwood number) in both highly curved and classical helixes. The proposed correlation (which is reported in Appendix B) is valid for $R_H^* \leq 10$, $p^* \leq 15$, Reynolds numbers, *Re*, ranging from 10 to 2 000, and Prandtl numbers, *Pr*, (respectively Schmidt numbers, *Sc*) between 1 and 10. With such relatively low values of *Pr*/*Sc*, entrance effects may be neglected in the case of pipes of small diameter and/or sufficient length, which is generally the case in the applications targeted in this study, namely micro-structured heat exchangers and monolith catalytic reactors. Accordingly, in these situations, the asymptotic Nusselt/Sherwood numbers that can be calculated using the correlation of Abushammala et al. (2020), allow representing the effective convective heat/mass transfer rate in the pipe, and therefore, they will be simply denoted *Nu* and *Sh* further on in this paper. It is worthy to note that for relatively high *Pr* or *Sc* numbers, as entrance lengths may become too important, the fully developed *Nu* / *Sh* values can no more correctly approximate the effective heat/mass transfer rates which will vary depending on the used pipe length (i.e. depending on the Graetz number). These situations will not be treated in the present paper which will only focus on working fluids with relatively low *Pr* and *Sc* values, i.e. lower than 10.

Figure 6a displays the contour plot, calculated using the correlation of Abushammala et al. (2020), of the Nu_H to Nu_S (respectively Sh_H to Sh_S) ratio for *Re* equal 2 000 and a *Pr* (respectively *Sc*) of 10, where the subscripts H and S respectively refer to helical and straight pipes. Note that *Nu*, *Sh* and *Re* are all defined upon the pipe diameter as characteristic length scale. This contour plot illustrates the heat/mass transfer enhancement that helical pipes allow in comparison to the base case. Note that Nu_S equals 3.66 since a laminar flow with an isothermal wall boundary condition is considered (while Nu_S would be equal to 4.36 under a uniform heat flux condition).

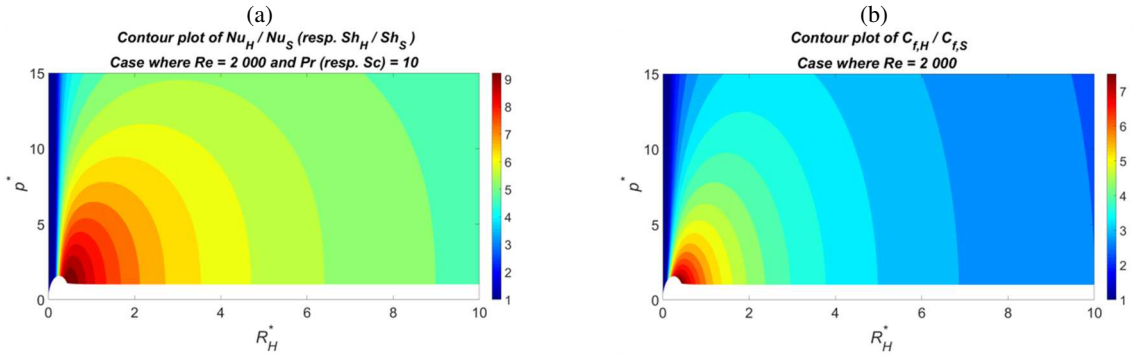

Figure 6: Example of contour plots in the (R_H^* , p^*) space of (a) the Nu_H to Nu_S (respectively Sh_H to Sh_S) ratio and (b) the $C_{f,H}$ to $C_{f,S}$ ratio, respectively calculated using the correlations of Abushammala et al. (2020) and Abushammala et al. (2019a). Note that a different scale is used for each subfigure.

As shown by Figure 6a, helical pipes lead to a significant improvement of the transfer efficiency, in particular highly curved ones which, thanks to the intense Deans vortices they develop, allow reaching heat/mass transfer rates nearly 9 times higher than straight pipes. However, these strong recirculations also induce higher mechanical energy dissipation per unit pipe length. Therefore, it is necessary to account for this friction coefficient increase in order to evaluate the cost-effectiveness of HCHP geometries.

Abushammala et al. (2019a) proposed a correlation for predicting the friction coefficient in both highly curved and classical helixes, under laminar flow conditions. The proposed correlation (which is reported in Appendix C) is valid for $R_H^* \leq 10$, $p^* \leq 20$ and *Re* ranging from 10 to 2 000. Figure 6b displays the contour plot, calculated using this correlation, of the $C_{f,H}$ to $C_{f,S}$ ratio (where C_f designates the friction coefficient in the case where *Re* equals 2 000. It can be noticed that helical pipes may lead to a significant friction coefficient increase, in particular highly curved ones, where the C_f may exceed by more than 7 times that of straight pipes. Therefore, in order to be able to assess the potentiality of HCHPs and other designs for process intensification of heat/mass exchangers, it is necessary to develop performance criteria simultaneously accounting for the heat/mass transfer enhancement, friction coefficient increase and packing density effects.

3. Alternative heat/mass transfer enhancement techniques

The present paper aims at evaluating the potentiality of helical pipes for heat/mass transfer intensification under laminar flow conditions, and comparing it to alternative enhancement strategies. This section reviews

literature studies (summarized in Table 1) dealing with alternative heat transfer enhancement techniques, in which both heat transfer and friction factor data were reported (to be able to assess the cost-effectiveness of the method used). To allow a reliable comparison, only studies with a Prandtl number comprised between 1 and 10 and Reynolds numbers below 2 000 are considered, which corresponds to the range of validity of the correlations presented in Section 2.2. Among the papers presenting novel pipe geometries, only those reporting the full geometric details of their designs have been considered. The maximum specific surface area of these designs has been determined using the CAD software Autodesk Inventor Professional 2018 assuming a triangular lattice arrangement (following the procedure presented in Abushammala et al. (2020)), and the results are reported in Table 1.

Based on CFD simulations, Wang et al. (2020) identified a novel coiled pipe design with a trilobal cross-section (which was called 'helically coiled-twisted trilobal tube', Figure 7a) allowing a significant heat transfer enhancement. They also carried out an experimental investigation to validate their numerical data. Compared to a classical helical pipe with a circular cross-section, the novel design was shown to further improve the Nusselt number at the inner tube side by 19% to 31%, while increasing the friction factor by 24% to 38%. However, because of its relatively large helix radius and moderate pitch, this novel geometry exhibits a low packing density. Thus, as reported in Table 1, the calculation of its maximal specific surface area shows that it is less than 25% of that developed by densely packed straight tubes of same - outer - diameter. This drawback limits the potential of this novel design for process intensification purposes as it will be discussed in Section 4.

Tohidi et al. (2015) investigated numerically the thermo-hydraulic performance of a helically coiled heat exchanger that induces a chaotic flow behavior. The novel design follows a helically coiled configuration, however its helix turns consist of alternating right-handed and left-handed helix segments (Figure 7b). Their numerical results revealed that, compared to a classical helical pipe, the novel geometry allows enhancing heat transfer by 4% to 26% for a friction coefficient increase of 5% to 8% only. Although Tohidi et al. (2015) claimed that their novel design exhibits a higher packing density than alternative chaotic heat exchangers, because of its relatively large helix radius and low helix pitch, its maximum specific surface area remains very low and is about 5 times smaller than that developed by densely packed straight tubes having the same pipe diameter (Table 1).

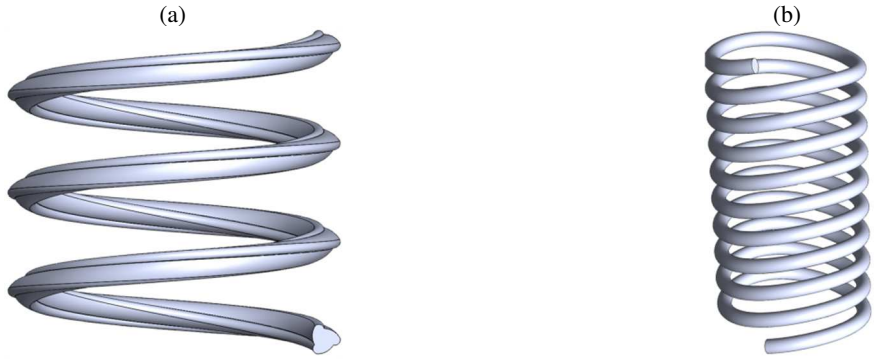

Figure 7: Schematic representations of the novel heat exchanger designs proposed by: (a) Wang et al. (2020), (b) Tohidi et al. (2015).

Table 1: Summary of studies dealing with alternative techniques of heat transfer enhancement under laminar flow conditions.

Reference	**Heat enhancement technique**	**Investigation technique**	**Wall thermal boundary condition**	***Pr***	$\frac{\sigma^*_{max}}{\sigma^*_{S,max}}$
Wang et al. (2020)	Twisted helical pipe with trilobal cross-section which was referred to as 'helically coiled-twisted trilobal tube' (Figure 7a)	Only their experimental result with *Re* = 2 000 is considered in this paper (their remaining data correspond to turbulent flows)	Uniform wall temperature	7	0.234

Kurnia et al. (2020)	Different twisted tapes fitted within a straight or a helical pipe	CFD	Uniform wall temperature	7	1 for the straight tube; 0.212 for the helical pipe
Khosravi-Bizhaem et al. (2019)	Four helical pipes were investigated under pulsating flow conditions	Experimental. For clarity purposes, only their results under a pulsating frequency of 4 Hz (which led to the best performance) are considered in this paper.	Uniform heat flux	5.5	0.110, 0.105, 0.071and 0.053 respectively for the four helical pipes
Tohidi et al. (2015)	Chaotic helically coiled geometry (Figure 7b)	CFD	Uniform heat flux	7	0.212
Guo et al. (2011)	Two different twisted tapes fitted within straight pipes	CFD	Uniform heat flux	7	1
Wongcharee and Eiamsa-Ard (2011)	Two different twisted tapes fitted within straight pipes	Experimental study	Uniform heat flux	7	1

Khosravi-Bizhaem et al. (2019) experimentally investigated the effects of pulsatile flow conditions on heat transfer enhancement in helical pipes. Four helix designs were used, all exhibiting a large helical radius and a small pitch, and thus, a very low specific surface area as reported in Table 1. Compared to steady-state operation, pulsatile flow conditions were shown to enable a significant improvement of the convective transfer rate, up to 39%, while the pressure drop was increased by 3% to 7% only. It is noteworthy that Khosravi-Bizhaem et al. (2019) mainly focused on turbulent flow conditions, although some of their data fall within the laminar flow regime (only these results are considered in the present paper). However, the accuracy of the manometer they used was not sufficient for precise measurements of the relatively low pressure drops occurring in the laminar flow experiments. Hence, many of their time-averaged pressure drop measurements under pulsatile conditions were even significantly lower than those predicted by correlations dealing with steady-state operation (Abushammala et al., 2019a; Hart et al., 1988; Mishra and Gupta, 1979). Therefore, their friction factor data should be considered with caution especially that, as shown later in Section 4, they seem to be largely underestimated as they lead to unrealistic cost-effectiveness performances.

Guo et al. (2011), Wongcharee and Eiamsa-Ard (2011) and Kurnia et al. (2020) have focused on heat transfer enhancement by twisted tapes fitted within straight tubes. All these studies agree that properly designed inserts allow impressive enhancement rates, although they generally lead to a significant pressure drop increase. Kurnia et al. (2020) also considered the situation where the twisted tapes are disposed within a helical pipe. This configuration enabled better enhancement rates than when the twisted tapes are fitted within a straight pipe, but it also led to higher pumping requirements.

4. Results and discussion

As mentioned in Section 1, performance evaluation criteria proposed thus far in literature do not account for specific surface area effects. Thus, in the case of heat/mass exchangers or reactors where a large number of flow tubes need to be used, these criteria are not relevant for characterizing the potential of novel designs or enhancement strategies in terms of process intensification, i.e. in terms of allowed unit volume reduction. Therefore, new performance evaluation indexes, following the general form given in Equation 6, are proposed in this paper (for heat and mass transfer situations respectively):

$$\theta_{1,n} = \frac{(\sigma^*_{max}\, Nu)/(\sigma^*_{S,max}\, Nu_S)}{\left(C_f/C_{f,S}\right)^n} \quad or \quad \theta_{1,n} = \frac{(\sigma^*_{max}\, Sh)/(\sigma^*_{S,max}\, Sh_S)}{\left(C_f/C_{f,S}\right)^n} \qquad \text{Eq. 6}$$

where θ is the intensification performance factor. n is a positive weighting factor expressing the relative weight accorded to pumping costs compared to the volumetric heat/mass transfer enhancement. Subscript S

refers to the base case of a smooth straight pipe under steady state operation. The numerator of Eq.6 represents the heat/mass transfer enhancement per unit volume that a given enhancement strategy allows achieving compared to the base case.

In the subsequent paragraphs, the potentiality of helical pipes is evaluated using different performance indexes following the general forms presented in Equations 1 and 6. For each considered criterion, some particular helix designs are shown to enable good to excellent performances. Elongated helixes and highly curved ones reveal to be particularly relevant for process intensification purposes, showing comparable or better performances than alternative enhancement techniques and designs.

4.1. Heat/Mass transfer enhancement per unit surface

A first criterion for evaluating the performances of helical pipes or alternative techniques is $\eta_{1,0}$ (following the general form given in Eq. 1), which simply corresponds to the Nu to Nu_S (respectively Sh to Sh_S) ratio, i.e. to the heat/mass transfer augmentation allowed by the considered technique in comparison to the base case. This criterion is relevant in situations where pumping costs are not an issue, for example when the working fluids are available at sufficient pressure. Since it does not account for specific surface area effects, the use of $\eta_{1,0}$ is relevant in situations where only a single flow tube is to be used and where space is not a major concern. For example, a $\eta_{1,0} = 2$ indicates that the enhancement strategy allows achieving a similar heat/mass flux than that obtained with the base case, while reducing the surface of the heat/mass transfer device (and so the purchased material mass) by a factor up to 2 (in particular when the heat/mass transfer resistance is mostly located at the inner side of the tube, and in the presence of a heterogeneous chemical reaction, if it is diffusion-controlled). Or alternatively, for a same exchange surface, a $\eta_{1,0} = 2$ means that the enhancement technique allows achieving a heat/mass flux that is up to twice that obtained with the base case.

As displayed in Figure 6a, among helical pipes, highly curved ones enable the best transfer efficiencies. However, the allowed enhancement rate depends on both Re and Pr (respectively Sc) values. In order to characterize the flow effects, the Reynolds number was varied from 10 to 2 000 using length steps of 10. At each Re value, using the correlation of Abushammala et al. (2020), $\eta_{1,0}$ was calculated for all helixes with $R_H^* \leq 10$ and $p^* \leq 15$, using length steps of 0.05 for varying both R_H^* and p^*.Then, at each Re, the maximal $\eta_{1,0}$ value that could be achieved by helical pipes was determined, and the geometric parameters of the helix allowing to achieve this optimal performance were identified. In order to characterize the fluid properties effects, this same procedure was performed for three Pr (respectively Sc) values: 1, 7 and 10. The calculation results are plotted in Figure 8. Plots on the upper graph display the maximal $\eta_{1,0}$ that can be achieved by helical pipes, depending on Re and Pr values. The discontinuity in the curves at Re = 400 is due to the fact that the correlation of Abushammala et al. (2020) (see Appendix B) relies on different mathematical expressions respectively when Re is higher or lower than 400. The middle and lower graphs in Figure 8 display the geometric parameters of the helixes achieving the maximal $\eta_{1,0}$ depending on Re and Pr (respectively Sc) conditions.

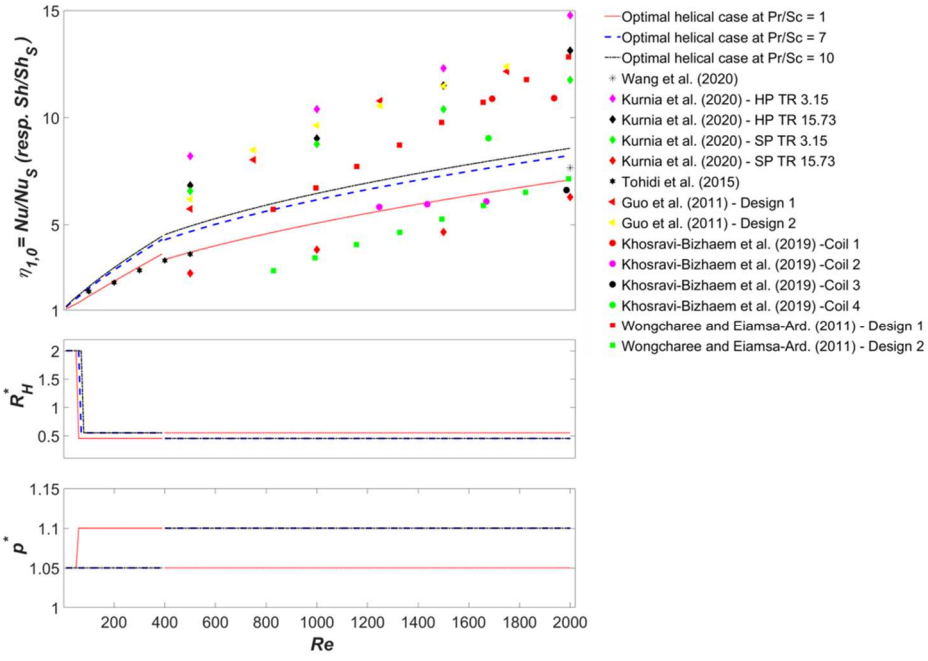

Figure 8: Performances of helical pipes and alternative enhancement techniques based on the $\eta_{1,0}$ criterion. In the figure caption, for the data of Kurnia et al. (2020), HP and SP respectively refer to the use of a helical or a straight pipe, while TR refers to the twist ratio of the used twisted tape.

As revealed by Figure 8, helical pipes allow a considerable improvement of heat/mass transfer with an enhancement rate exceeding 9 at Re = *2 000* and Pr (respectively Sc) = 10. Optimal helixes performances are always achieved by HCHPs having a R_H^* between 0.4 and 2 and a p^* of about 1.1. When Re increases, centrifugal effects become higher and lead to more intense Dean vortices. Therefore, enhancement capacities of helical pipes improve with increasing Re.

For comparison purposes, literature data (refer to Table 1 and Section 3 for details) are also plotted in Figure 8. It can be noticed that HCHPs allow better performance than the designs proposed by Wang et al. (2020) and Tohidi et al. (2015) (their data were acquired using water at Pr = 7) which are based on a modified 'classical' helical geometry. However, if the design modifications proposed by these authors were applied to HCHPs, it is possible that they would have yielded much better performances.

Pulsatile helical pipe flows, investigated by Khosravi-Bizhaem et al. (2019), allow obtaining better performance than HCHPs in some situations, depending on the 'classical' helical pipe geometry studied. Given that these authors reported significant enhancement compared to steady state operation, the application of pulsatile flow to HCHPs is worthy of investigation as it could allow a substantial further improvement of their efficiency.

The data of of Guo et al. (2011), Wongcharee and Eiamsa-Ard (2011) and Kurnia et al. (2020) correspond to the use of twisted tapes. They reveal that, while inadequately designed internals lead to relatively poor performances, correctly conceived twisted tapes allow achieving impressive enhancement factors, much better than those obtained with HCHPs. The twisted tape with a twist ratio of 3.15 that has been investigated by Kurnia et al. (2020), when fitted within a helical pipe, displays the best efficiency among the augmentation techniques addressed in this paper. For Re = 2 000 and Pr = 7, it allows enhancing the convective transfer rate by nearly 15-fold.

4.2. Volumetric heat/mass transfer enhancement

As it does not account for specific surface area effects, the $\eta_{1,0}$ criterion is not relevant for evaluating the potentiality of helical pipes or alternative techniques for process intensification, in particular in situations where a large number of flow tubes need to be packed. Such processes include monolith catalytic reactors and printed-circuit heat exchangers, where a dense packing of the flow tubes (i.e. a high specific surface area) is necessary to minimize the volume of the heat/mass exchanger.

A convenient criterion in such situations is $\theta_{1,0}$ (following the general form given in Eq. 6) which is defined as follows (for heat and mass transfer situations respectively):

$$\theta_{1,0} = \frac{\sigma^*_{max}\, Nu}{\sigma^*_{S,max}\, Nu_S} \quad or \quad \theta_{1,0} = \frac{\sigma^*_{max}\, Sh}{\sigma^*_{S,max}\, Sh_S} \qquad \text{Eq. 7}$$

$\theta_{1,0}$ represents the ratio of the volumetric heat/mass flux allowed by a given technique/design to that achieved by the base case. For example, a $\theta_{1,0}$ = 2 indicates that the enhancement strategy allows obtaining a similar heat/mass flux than the base case while allowing to reduce the volume of the heat/mass transfer device up to a factor 2 (in particular when the heat/mass transfer resistance is mostly located at the inner side of the tube, and in processes involving a heterogeneous chemical reaction, if the reaction is diffusion-controlled). Thus, $\theta_{1,0}$ quantifies the potentiality for miniaturization of an enhancement strategy or design. Since it does not account for the friction coefficient increase, this criterion is relevant in situations where the available space is the only primary concern.

Figure 9 displays contour plots in the (R_H^* , p^*) space of the $\theta_{1,0}$ criterion for Pr (respectively Sc) = 10 and Re = 100 and 2 000 (note that different scales are used for figures a and b). They are calculated using the correlations of Abushammala et al. (2020) whence the discontinuity at R_H^* = 2 (see Section 2.1). These results reveal that, given their high transfer rate (Figure 6a) and specific surface area (Figure 5b), HCHPs allow tremendous enhancements of volumetric transfer rates. The performances of HCHPs improve with increasing Re as Dean vortices become more and more intense. Hence, for Re = 2 000 and Pr (respectively Sc) = 10, HCHPs enable a great volume reduction of heat/mass exchangers with more than an 8-fold factor. On the other hand, in the case of 'classical' helical pipes, the provided heat/mass transfer enhancement remains limited and is not always sufficient to compensate the effects of their low packing densities. Hence, 'classical' helical pipes may perform even worse than straight tubes (i.e. $\theta_{1,0}$ values lower than one), in particular under low Re conditions.

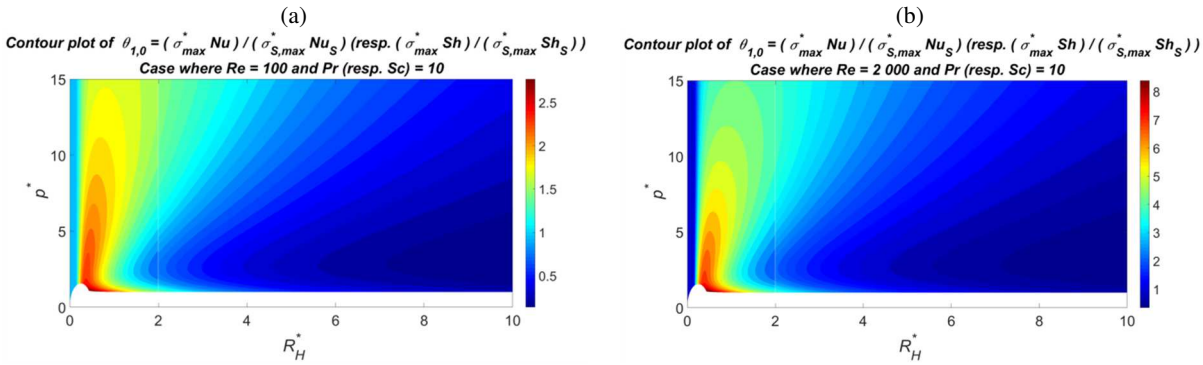

Figure 9: Contour plots in the (R_H^* , p^*) of the $\theta_{1,0}$ criterion for: (a) Re = 100 and Pr/Sc = 10. (b) Re = 2 000 and Pr/Sc = 10.

Figure 10 displays the maximal $\theta_{1,0}$ that can be achieved by helical pipes depending on Re and Pr (respectively Sc) conditions. The discontinuity in the curves at Re = 400 is due to the fact that the correlation of Abushammala et al. (2020) for calculating Nu (respectively Sh) relies on different mathematical expressions depending on whether Re is higher or lower than 400. It can be noticed from this figure that, apart from very low Re values, optimal performances are always achieved by HCHPs having a R_H^* between 0.4 and 0.6 and a p^* of about 1.1. In addition, HCHPs intensification potentiality increases with increasing Re and Pr (respectively Sc).

For comparison with helical pipe designs, the $\theta_{1,0}$ performance of alternative enhancement methods is also displayed in Figure 10. Because of the low specific surface area they develop, all the designs and techniques based on 'classical' helical pipe geometries exhibit much inferior performances than HCHPs, and some perform even worse than straight tubes. On the other hand, correctly designed twisted tapes disposed in straight tubes offer impressive intensification potentials, appreciably higher that those obtained with HCHPs. Indeed, on the one hand, twisted tapes lead to great transfer rates (Section 4.1), while the straight tube geometry allows developing a high specific surface area. Thus, twisted tapes seem to constitute the most efficient solution for the miniaturization of heat/mass transfer devices. One may wonder if the use of twisted tapes within HCHPs would not allow obtaining even higher intensification potentialities. Finally, it should be kept in mind that twisted tapes present some drawbacks which may limit their usage in some situations. In particular, as they are subject to fouling and scaling, they may lead to significant maintenance and cleaning costs.

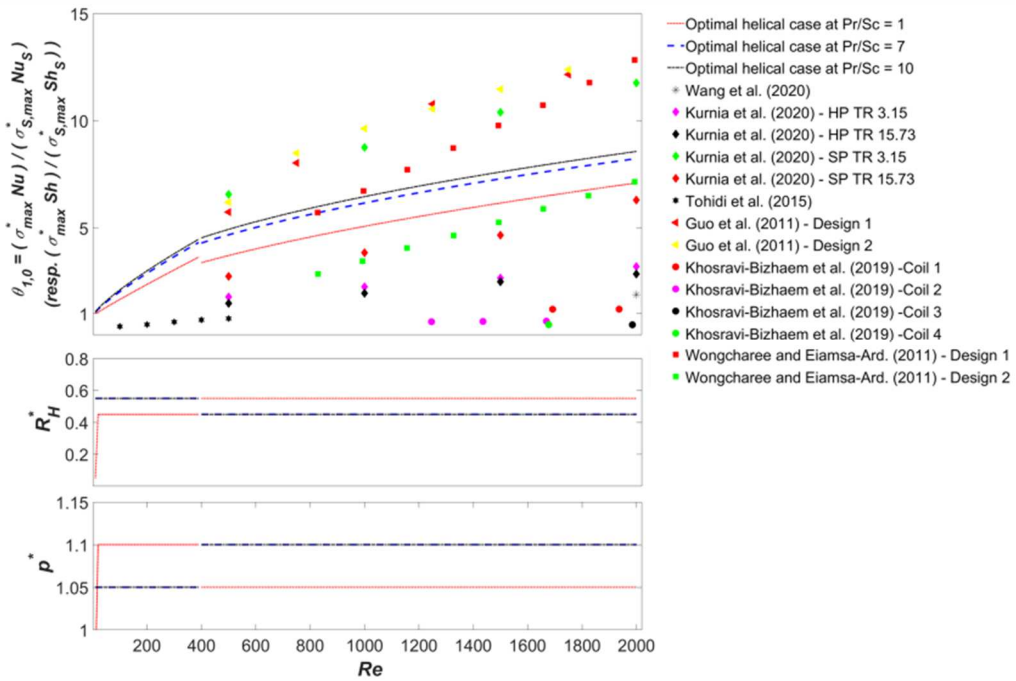

Figure 10: Performances of helical pipes and alternative enhancement techniques based on the $\theta_{1,0}$ criterion. In the figure caption, for the data of Kurnia et al. (2020), HP and SP respectively refer to the use of a helical or a straight pipe, while TR refers to the twist ratio of the used twisted tape.

In addition, it is worthy to note that compared to straight tubes with (or without) inserts, helical pipes are expected to allow better transfer rates at the external side of the tubes (although this would require higher pumping power for the external fluid flow). This advantage of helical pipes over straight ones may be of primary importance in applications where both external and internal transfer limitations exist. However, for quantifying such effects, general correlations for predicting transfer rates and friction coefficients at the external flow side of helical tubes are required. To the authors best knowledge, so far, no such correlation has been proposed in the literature.

4.3. Cost-effectiveness of heat/mass transfer enhancement per unit surface

The criteria that have been examined in the previous sections are relevant when the minimization of the exchanger/reactor surface or volume is the sole main objective, while pumping power concerns can be omitted. However, in most situations, to be of industrial relevance, enhancement methods and designs should allow a good trade-off between the minimization of both operating (i.e. pumping power) and purchase (i.e. material mass) costs. One appropriate criterion than enables to simultaneously account for these two conflicting objectives is $\eta_{1,1}$ which is expressed in Eq. 2. $\eta_{1,1}$ can be seen as an assessment of the cost-effectiveness of enhancement methods and designs aiming at minimizing exchangers surface.

Figure 11 presents contour plots in the (R_H^* , p^*) space of the $\eta_{1,1}$ criterion for Pr (respectively Sc) = 10 and Re = 100 and 2 000. Both Nu (respectively Sh) and C_f are calculated using the correlations of Abushammala et al. (2020, 2019a) (see Section 2.1). Figure 12 displays the maximal $\eta_{1,1}$ that can be achieved by helical pipes depending on Re and Pr (respectively Sc) conditions.

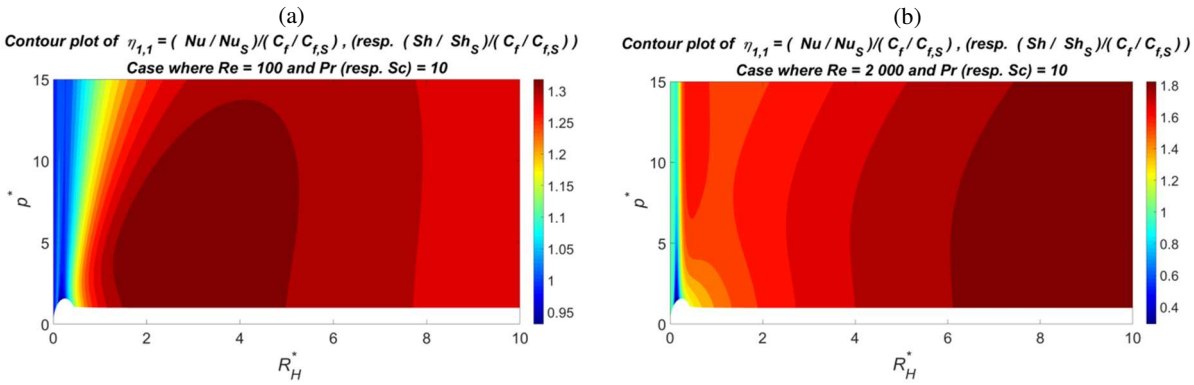

Figure 11: Contour plots in the (R_H^* , p^*) of the $\eta_{1,1}$ criterion for : (a) Re = 100 and Pr/Sc = 10 (b) Re = 2 000 and Pr/Sc = 10.

Figures 11 and 12 reveal that optimal performances in terms of $\eta_{1,1}$ criterion are not achieved by HCHPs, but rather by 'classical' helixes. Indeed, as can be seen from Figures 6a and 6b, although HCHPs do lead to great transfer rates, they also induce relatively high friction losses. On the other hand, it can be noticed that the heat/mass transfer enhancement provided by 'classical' helical pipes is significantly higher than the friction coefficient increase they induce.

Figure 12 indicates that at relatively low Reynolds numbers, optimal $\eta_{1,1}$ values are achieved by helixes having a R_H^* of about 2 and a moderate to high p^*. On the other hand, for relatively high Reynolds numbers, the highest $\eta_{1,1}$ values are obtained with helixes of low p^* and a large R_H^* of 10, which is the highest R_H^* value considered in this study. The significant discontinuity appearing at Re = 400 is due to several reasons. First, the fact that both correlations calculating C_f (Abushammala et al., 2019a) and Nu (respectively Sh) (Abushammala et al., 2020) rely on different mathematical expressions depending on whether Re is higher or lower than 400. Second, as can be seen from Figures 11a and 11b, for a given Re, there is a large range of geometric parameters R_H^* and p^* where helixes achieve high performances. From an engineering point of view, given the limited precision of any correlation, all of these helixes can be regarded as exhibiting high and similar efficiencies. However, mathematically speaking, the exact R_H^* and p^* coordinates of the helix achieving the highest $\eta_{1,1}$ value may be indeed very sensitive to the correlation expression used, whence the significant discontinuity appearing at Re = 400.

Finally, it is noteworthy that, even with the relatively low Pr (respectively Sc) numbers considered in this study, most helical designs allow obtaining $\eta_{1,1}$ values higher than unity (Figure 11), which means that the heat/mass enhancement they provide is higher than the friction coefficient increase they induce. This point is of major importance from a cost-efficiency perspective. Indeed, for achieving a given heat/mass flux, by virtue of

their higher *Nu* (resp. *Sh*), helical tubes require a shorter pipe length than the base case. The fact that their $\eta_{1,1}$ value is higher than unity implies that the effect of their shorter length on pumping power overcomes the effect of their higher friction coefficient. Thus, helical pipes prove to be a cost-effective solution that, compared to the base case, allows simultaneously reducing the exchanger surface and the associated pumping costs. Obviously, this conclusion is valid as long as the heat/mass transfer is limited by the convective resistance at the inner flow side.

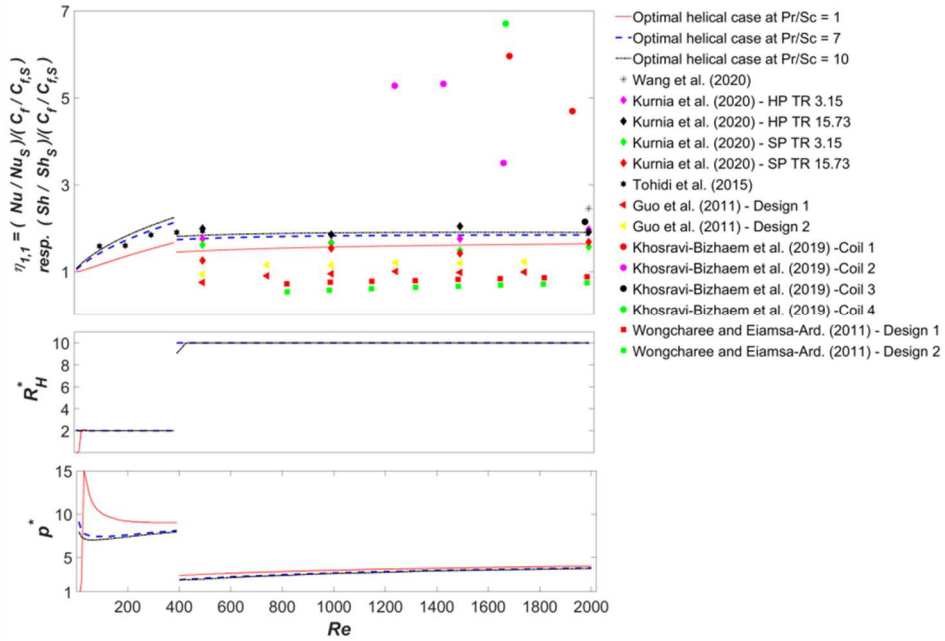

Figure 12: Performances of helical pipes and alternative enhancement techniques based on the $\eta_{1,1}$ criterion. In the figure caption, for the data of Kurnia et al. (2020), HP and SP respectively refer to the use of a helical or a straight pipe, while TR refers to the twist ratio of the used twisted tape.

Comparison between helical pipes and alternative techniques is carried out in Figure 12. The data of Khosravi-Bizhaem et al. (2019) suggest that pulsating flow conditions allow achieving remarkably higher performances than the remaining methods. However, as noted in Section 3, pressure drop measurements performed by these authors have probably largely underestimated the friction coefficient which leads to these surprising results.

Twisted tapes disposed in straight tubes exhibit slightly to much lower performances than helical pipes in terms of $\eta_{1,1}$ criterion. Indeed, although they lead to tremendous enhancement rates (Figure 8), they also induce excessive frictional losses.

On the other hand, enhancement methods based upon a helical design constitute energy-efficient solutions for heat/mass transfer augmentation. Hence, the chaotic heat exchanger of Tohidi et al. (2015) and the twisted tapes fitted within a helical tube of Kurnia et al. (2020) display similar performances than helical pipes. The geometry proposed by Wang et al. (2020) seems to be the most effective with regard to the $\eta_{1,1}$ criterion. Unfortunately, these authors mainly focused on turbulent flows and performed a single experimental measurement within the laminar regime (at a *Re* of about 2 000, see Figure 12) only, which limits the comparison.

4.4. Cost-effectiveness of volumetric heat/mass transfer enhancement

As it does not account for specific surface area effects, the $\eta_{1,1}$ criterion is not relevant for evaluating the potentiality of helical pipes or alternative techniques for cost-effective process intensification, in particular in situations where a large number of flow tubes need to be used. Such processes include monolith catalytic reactors and printed-circuit heat exchangers, where a dense packing of the flow tubes (i.e. a high specific surface areas) is necessary for minimizing the volume of the heat/mass exchanger.

A convenient criterion in such situations is $\theta_{1,1}$ which is defined as follows (for heat and mass transfer situations respectively):

$$\theta_{1,1} = \frac{(\sigma^*_{max}\, Nu \,/\, C_f)}{(\sigma^*_{S,max}\, Nu_S /\, C_{f,S})} \quad or \quad \theta_{1,1} = \frac{(\sigma^*_{max}\, Sh \,/\, C_f)}{(\sigma^*_{S,max}\, Sh_S /\, C_{f,S})} \qquad \text{Eq. 8}$$

$\theta_{1,1}$ compares the volumetric heat/mass transfer enhancement allowed by a given strategy to the relative friction coefficient increase that it induces with respect to the base case. Thus, it allows evaluating the potentiality of a given method in terms of cost-effective miniaturization.

Figure 13 presents contour plots in the (R_H^* , p^*) space of the $\theta_{1,1}$ criterion for Pr (resp. Sc) = 10 and Re = 100 and 2 000 respectively. The geometric features and thermo-hydraulic performances of helical pipes, σ_{max}^*, Nu (resp. Sh) and C_f, were calculated using the correlations of Abushammala (2019a, 2020) (that are reported in Appendices A, B and C). Figure 14 displays the maximal $\theta_{1,1}$ that can be achieved by helical pipes depending on Re and Pr (resp. Sc) conditions.

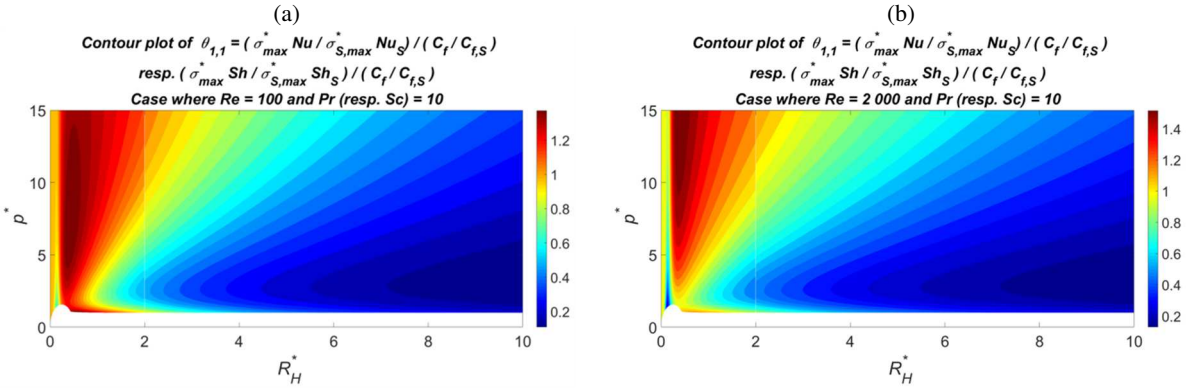

Figure 13: Contour plots in the (R_H^* , p^*) of the $\theta_{1,1}$ criterion for: (a) Re = 100 and Pr/Sc = 10 (b) Re = 2 000 and Pr/Sc = 10.

Figures 13 and 14 reveal that the best $\theta_{1,1}$ performances are achieved by helixes having a low R_H^* and a relatively high p^*. These designs provide the finest trade-off between a high specific surface area (Figure 5b), a good convective transfer rate (Figure 6a) and a relatively low friction coefficient (Figure 6b). At high Re values, maximal performances are reached with helixes of p^* = 15, which is the highest p^* value investigated in this study.

These results reveal that elongated helixes of low R_H^* allow achieving $\theta_{1,1}$ values higher than unity. Thus, these helix designs are particularly appropriate for conceiving compact units. Indeed, compared to the base case, they simultaneously enable to decrease the required pumping power and to considerably reduce the volume of the heat/mass exchanger or reactor. This conclusion remains valid as long as the heat/mass transfer is limited by the convective resistance at the inner flow side.

Comparison with literature data is carried out in Figure 14 which shows that all methods based on a 'classical' helix geometry poorly perform with respect to the $\theta_{1,1}$ criterion because of the low specific surface area they develop. Despite their high packing density and convective transfer rate, straight tubes equipped with twisted tapes generally exhibit much lower performances than helical pipes because of the significant friction losses they induce. Only those investigated by Kurnia et al. (2020) achieve comparable or slightly higher potentialities than elongated helix designs.

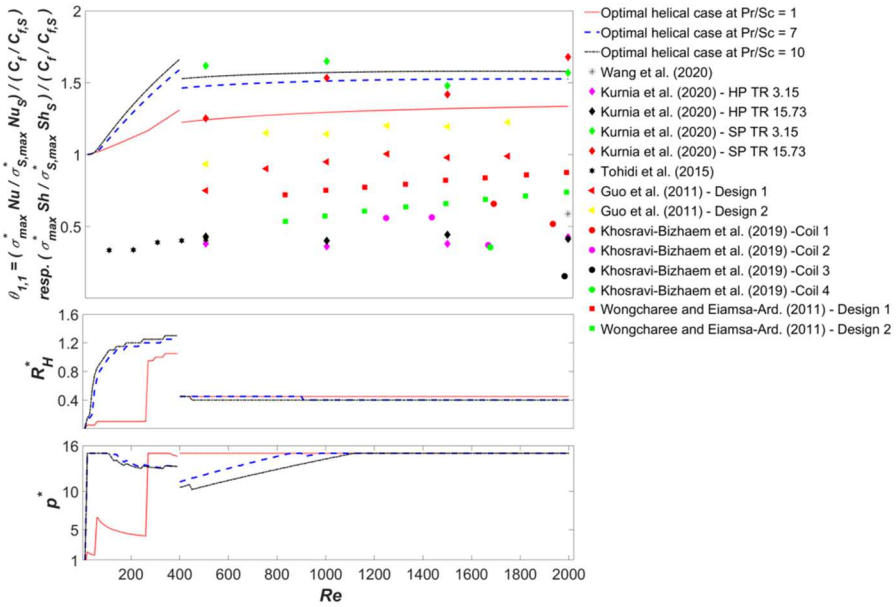

Figure 14: Performances of helical pipes and alternative enhancement techniques based on the $\theta_{1,1}$ criterion. In the figure caption, for the data of Kurnia et al. (2020), HP and SP respectively refer to the use of a helical or a straight pipe, while TR refers to the twist ratio of the used twisted tape.

4.5. Cost-effectiveness of volumetric heat/mass transfer enhancement in 'shell-and-tube' configurations

As discussed in the previous section, in many applications (e.g. monolith catalytic reactors, printed-circuit heat exchangers), the flow tubes need to be packed as densely as possible in order to minimize the exchanger volume. However, in many other processes, two fluids need to be used, one circulating within the tubes and the other within a shell. Such processes include shell-and-tube heat exchangers, hollow fiber dense membrane contactors, multitubular and monolithic catalytic reactors where temperature is regulated using a heating or cooling fluid, etc.

In such configurations, the tubes packing density should be carefully fixed so as to ensure a good trade-off between intensification purposes and a limited pressure drop at the shell-side. Attributing half of the unit volume to the fluid circulating within the tubes is a good compromise, the remaining half volume being left for the tubes walls and to the fluid circulating within the shell. Thus, at a first approximation, it may be considered that a packing density of 0.5 is the most appropriate in such configurations. As mentioned in Section 2.1, the maximal packing density of cylinders is 90.7%, and their dimensionless specific surface area under these dense packing conditions is noted $\sigma^*_{S,max}$. Thus, under a packing density of 50%, the specific surface area developed by straight tubes equals (0.5/0.907)×σ^*_{max} = 0.55 σ^*_{max}. Accordingly, a new criterion, $\chi_{1,1}$, is proposed for assessing the cost-effectiveness of volumetric heat/mass transfer enhancement in exchangers following a shell-and-tube configuration:

$$\chi_{1,1} = \begin{cases} \dfrac{(\sigma^*_{max}\, Nu\,/\,C_f)}{(0.55\,\sigma^*_{S,max}\, Nu_S/\,C_{f,S})} = \dfrac{\theta_{1,1}}{0.55} \quad or \quad \dfrac{(\sigma^*_{max}\, Sh\,/\,C_f)}{(0.55\,\sigma^*_{S,max}\, Sh_S/\,C_{f,S})} = \dfrac{\theta_{1,1}}{0.55} & if\ \phi_{max} \le 0.5 \\ \dfrac{(\sigma^*_{0.5}\, Nu\,/\,C_f)}{(0.55\,\sigma^*_{S,max}\, Nu_S/\,C_{f,S})} \quad or \quad \dfrac{(\sigma^*_{0.5}\, Sh\,/\,C_f)}{(0.55\,\sigma^*_{S,max}\, Sh_S/\,C_{f,S})} & if\ \phi_{max} \ge 0.5 \end{cases} \qquad \text{Eq. 9}$$

With the $\chi_{1,1}$ criterion, the performances of an enhancement technique/design are compared to that of straight tubes disposed with a packing density of 50%, i.e. developing 55% of their highest possible specific surface area, whence the factor 0.55 at the denominator. Designs which maximal packing density is lower than 50% are considered to be packed as densely as possible (i.e. under their maximal possible packing density) since anyway, enough space would be left for the fluid circulating in the shell. On the other hand, geometries which maximal packing density exceeds 50% are considered to be arranged with a packing density of 50% only (and the dimensionless specific surface area they develop is noted $\sigma^*_{0.5}$) so as to keep a sufficient space for the fluid circulating at the shell side.

The ratio of the specific surface areas developed by helixes and straight tubes is equal to the ratio of their packing densities (see Eq. 5). Therefore, in the case of helical pipes, the expression of the $\chi_{1,1}$ criterion may be simplified and becomes:

$$\chi_{1,1} = \begin{cases} \dfrac{(\sigma^*_{H,max}\, Nu_H \,/\, C_{f,H})}{(0.55\, \sigma^*_{S,max}\, Nu_S/\, C_{f,S})} = \dfrac{\theta_{1,1}}{0.55} \quad or \quad \dfrac{(\sigma^*_{H,max}\, Sh_H \,/\, C_{f,H})}{(0.55\, \sigma^*_{S,max}\, Sh_S/\, C_{f,S})} = \dfrac{\theta_{1,1}}{0.55} & if\ \phi_{H,max} \leq 0.5 \\ \dfrac{(Nu_H \,/\, C_{f,H})}{(Nu_S/\, C_{f,S})} = \eta_{1,1} \quad or \quad \dfrac{(Sh_H \,/\, C_{f,H})}{(Sh_S/\, C_{f,S})} = \eta_{1,1} & if\ \phi_{H,max} \geq 0.5 \end{cases} \qquad \text{Eq. 10}$$

One can notice from Equation 10 that for helixes exhibiting a maximal packing density higher than 0.5, the expression of $\chi_{1,1}$ becomes the same as that of $\eta_{1,1}$ (Equation 2 and Section 4.3).

Figure 15 presents the contour plot in the (R^*_H , p^*) space of the $\chi_{1,1}$ criterion for *Pr* (resp. *Sc*) = 10 and *Re* = 2 000, and Figure 16 displays the maximal $\chi_{1,1}$ that can be achieved by helical pipes, depending on *Re* and *Pr* (resp. *Sc*) conditions. It can be noticed that the highest performances are achieved by elongated helixes having a low to moderate R^*_H value and a relatively high p^*, up to 15, the maximal p^* value considered in this investigation.

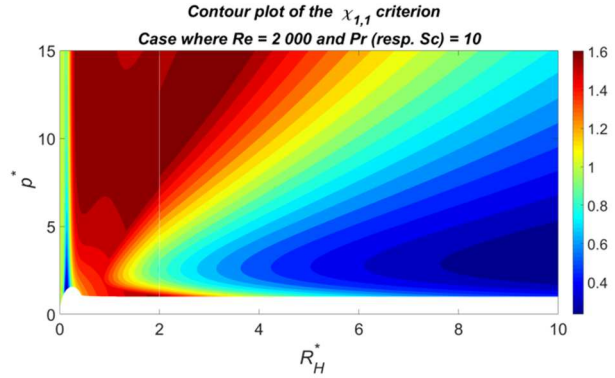

Figure 15: Contour plot in the (R^*_H , p^*) of the $\chi_{1,1}$ criterion for *Re* = 2 000 and *Pr*/*Sc* = 10.

The performances of alternative techniques are represented in Figure 16. Despite that with the $\chi_{1,1}$ criterion, the packing density of straight tubes is limited to 55% of its maximal possible value, methods based on a 'classical' helix geometry still exhibit relatively low performances because of their very low specific surface area, and generally achieve $\chi_{1,1}$ values lower than unity.

On the other hand, as straight tubes lose the advantage of their higher specific surface area, twisted tapes fitted within straight pipes achieve significantly to slightly lower $\chi_{1,1}$ performances than helical pipes. Hence, elongated helical designs allow achieving the highest $\chi_{1,1}$ values and reveal to be the most effective method for an energy-efficient miniaturization of exchangers following a shell-and-tube configuration.

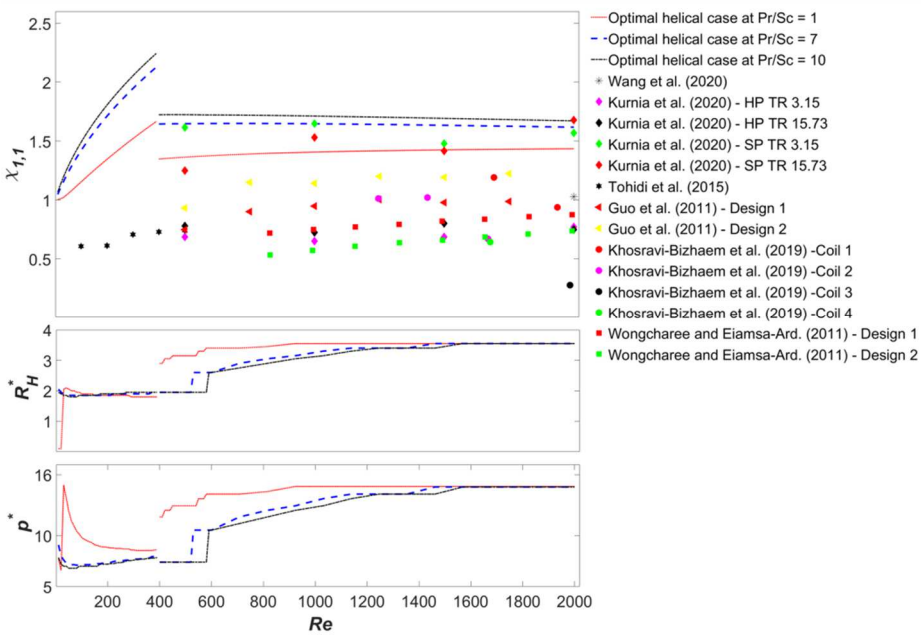

Figure 16: Performances of helical pipes and alternative enhancement techniques based on the $\chi_{1,1}$ criterion. In the figure caption, for the data of Kurnia et al. (2020), HP and SP respectively refer to the use of a helical or a straight pipe, while TR refers to the twist ratio of the used twisted tape.

5. Conclusion and perspectives

Novel performance criteria accounting for specific surface area effects have been proposed in this paper for evaluating the intensification potentiality of heat/mass transfer enhancement techniques. For each considered criterion, some particular helix designs have been shown to exhibit good to excellent performances. Highly curved helical pipes reveal to be a very efficient strategy for minimizing the volume of heat/mass exchangers and reactors. However, these geometries induce significant friction losses. On the other hand, elongated helical pipes of low helical radius were shown to allow cost-effective process intensification as they simultaneously enable to decrease the required pumping power and to considerably reduce the volume of reactors and heat/mass exchangers.

The performances of alternative techniques of heat/mass transfer enhancement (twisted tape inserts, pulsatile flow operation, and modified helical geometries) have also been analyzed, highlighting the weaknesses and strengths of each strategy. Applying these methods in conjunction with a highly curved or elongated helical design could allow a further improvement of their potentialities. This remains an open question that is worthy of deep investigation in future studies.

Acknowledgment

The authors gratefully thank the 'French ministry of higher education and research' for funding this study.

Nomenclature

a_{min}	Distance separating two closely packed helixes or straight tubes (m)
C_f	Friction coefficient following Darcy-Weisbach definition (-)
d	Pipe diameter (m)
n	Weighting factor (-)
Nu	Nusselt number (-)
p	Helix pitch (m)
Pr	Prandtl number (-)
R_H	Helix radius (m)
Re	Reynolds number (-)
s	Surface-to-volume ratio of a single pipe (m^{-1})
Sc	Schmidt number (-)
Sh	Sherwood number (-)

Greek letters

η	Performance evaluation criterion following the definition given in Equation 1 (-)
θ	Performance evaluation criterion following the definition given in Equations 7 or 8 (-)
γ	Radius of curvature of the pipe (m)
κ	Pipe curvature (m^{-1})
σ	Specific surface area of packed pipes (m^{-1})
ϕ	Packing density (-)
χ	Performance evaluation criterion following the definitions given in Equations 9 or 10 (-)

Subscripts

H	Refers to a helical pipe.
S	Refers to a smooth straight pipe under steady operation

Superscripts

*	Designates a dimensionless number

Appendix A

The correlation developed by Abushammala et al. (2020) for determining a^*_{min} in the case of helical pipes is given as follows:

where:

$$a^*_{min} = 1 + A\,tanh\left(B\ \ p^{*C}\right)$$
$$A = p_1\,R^*_H + p_2$$
$$B = p_3\,R^{*p_4}_H$$
$$C = p_5\,\ln(\,R^*_H\,) + p_6 \qquad \text{Eq. A.1}$$

The values of the parameters p_i are reported in Table A.1. Note that two different sets of values are used depending on whether R^*_H is lower or higher than 2.

Table A.1: Values of the parameters used in the correlation expressed by Eq. A.1.

Validity range	p_1	p_2	p_3	p_4	p_5	p_6
$0 \le R^*_H \le 2$	1.88	-5.54×10^{-2}	3.50	5.65×10^{-1}	-1.65×10^{-2}	-1.50
$2 \le R^*_H \le 10$	2.04	-3.65×10^{-1}	4.44	0	1.35×10^{-1}	-1.52

Appendix B

The correlation developed by Abushammala et al. (2020) for calculating the Nusselt number in helical pipe flows under laminar regime and isothermal wall conditions is given as follows:

where:

$$Nu_H = \frac{h\,d}{\lambda} = 3.657 + p_1\,A^{p_2}\,Re^B\,Pr^{p_7}\,exp(-C)$$
$$A = \left[R^*_H\left(1 + \left(\frac{p^*}{2\pi R^{*p_3}_H}\right)^{p_4}\right)\right]^{-1} \qquad \text{Eqs. B.1}$$
$$B = p_5\,Pr^{p_6}$$
$$C = p_8\,R^{*p_9}_H\,Pr^{p_{10}}$$

where the term 3.657 corresponds to the Nusselt number in straight tubes. h is the heat transfer coefficient, d the pipe diameter and λ the fluid thermal conductivity. The values of the parameters p_i are reported in Table B.1. Note that two different sets of values are used depending on whether Re is lower or higher than 400.

Table B.1: Values of the parameters used in the correlation expressed by Eq. B.1.

Validity range					
$10 \leq Re \leq 400$	p_1	p_2	p_3	p_4	p_5
	3.73×10^{-2}	3.81×10^{-1}	9.50×10^{-1}	2.64	9.38×10^{-1}
	p_6	p_7	p_8	p_9	p_{10}
	-7.09×10^{-2}	5.71×10^{-1}	6.43×10^{-2}	-1.15	3.84×10^{-1}
$400 \leq Re \leq 2\,000$	p_1	p_2	p_3	p_4	p_5
	3.03×10^{-2}	2.82×10^{-1}	7.19×10^{-1}	2.62	5.7×10^{-1}
	p_6	p_7	p_8	p_9	p_{10}
	-9.01×10^{-2}	4.35×10^{-1}	1.01×10^{-2}	-3.13	-1.32×10^{-1}

Equation B.1 also applies for determining the convective mass transfer rate in helical pipes by replacing *Nu* by *Sh* and *Pr* by *Sc*. Indeed, the heat/mass transfer analogy stipulates that *Nu* = *Sh* if *Pr* = *Sc*. The conditions for which this analogy holds are presented in Abushammala et al. (2020) and specialized textbooks.

Appendix C

The correlation developed by Abushammala et al. (2019a) for determining the friction coefficient, C_f, under laminar helical pipe flows is given as follows:

$$C_{f,H} = \frac{64}{Re} + A \,.\, B \,.\, \exp(-C)$$

where:

$$A = p_1 \,.\, D \,.\, \left(\frac{D}{Re}\right)^{p_2}$$

$$B = \left(R_H^* + \frac{1}{R_H^*}\right)^{p_3} \qquad \text{Eqs. C.1}$$

$$C = p_4 \,.\, D \,.\, p^* .\, R_H^{*-p_5}$$

$$D = \left[R_H^{*p_6}\left(1 + \left(\frac{p^*}{2\pi R_H^*}\right)^2\right)\right]^{-p_7}$$

where the term 64/*Re* corresponds to the friction coefficient in straight tubes (following the Darcy-Weisbach definition). The values of the parameters p_i are reported in Table C.1. Note that two different sets of values are used depending on whether *Re* is lower or higher than 400.

Table C.1: Values of the parameters used in the correlation expressed by Eq. C.1.

Validity range	p_1	p_2	p_3	p_4	p_5	p_6	p_7
$10 \leq Re \leq 400$	1.98	4.07×10^{-1}	8.49×10^{-1}	8.71×10^{-2}	8.91×10^{-1}	2.31	3.67×10^{-1}
$400 \leq Re \leq 2\,000$	2.88	3.82×10^{-1}	9.16×10^{-3}	2.48×10^{-3}	2.62	1.10	3.23×10^{-1}

References

Abushammala O., Hreiz R., Lemaitre C., Favre É., 2019a. Lami□ar flow frictio□ factor i□ highly curved helical pipes: Numerical i□vestigatio□, predictive correlatio□ a□d experime□tal validatio□ usi□g a 3D-pri□ted model. Chemical E□gi□eeri□g Scie□ce, 207, 1030-1039.

Abushammala O., Hreiz R., Lemaitre C., Favre, É, 2019b. Maximizi□g Mass Tra□sfer Usi□g Highly Curved Helical Pipes: A CFD I□vestigatio□. The 6th I□ter□atio□al Co□fere□ce of Fluid Flow, Heat a□d Mass Tra□sfer, Ju□e 2019.

Abushammala O., Hreiz R., Lemaitre C., Favre É., 2020. Optimal desig□ of helical heat/mass excha□gers u□der lami□ar flow: CFD i□vestigatio□ a□d correlatio□s for maximal tra□sfer efficie□cy a□d process i□te□sificatio□ performa□ces. I□ter□atio□al Jour□al of Heat a□d Mass Tra□sfer, 153, 119610.

Alam T., Kim M. H., 2018. A comprehe□sive review o□ si□gle phase heat tra□sfer e□ha□ceme□t tech□iques i□ heat excha□ger applicatio□s. Re□ewable a□d Sustai□able E□ergy Reviews, 81, 813-839.

Bhadouriya R., Agrawal A., Prabhu S. V., 2015. Experime□tal a□d □umerical study of fluid flow a□d heat tra□sfer i□ a□ a□□ulus of i□□er twisted square duct a□d outer circular pipe. I□ter□atio□al Jour□al of Thermal Scie□ces, 94, 96-109.

Dea□, W. R., 1927. Note o□ the motio□ of fluid i□ a curved pipe. Philosophical Magazi□e a□d Jour□al of Scie□ce, 4(20), 208-223.

Dea□, W. R., 1928. The stream-li□e motio□ of fluid i□ a curved pipe. Philosophical Magazi□e a□d Jour□al of Scie□ce, 5(30), 673-695.

Guo J., Fa□ A., Zha□g X., Liu W., 2011. A □umerical study o□ heat tra□sfer a□d frictio□ factor characteristics of lami□ar flow i□ a circular tube fitted with ce□ter-cleared twisted tape. I□ter□atio□al Jour□al of Thermal Scie□ces, 50(7), 1263-1270.

Hart J., Ellenberger J., Hamersma P. J., 1988. Single-and two-phase flow through helically coiled tubes. Chemical Engineering Science, 43(4), 775-783.

Kaufhold D., Kopf F., Wolff C., Beutel S., Hilterhaus L., Hoffmann M., Beutel S., Hilterhaus L., Hoffmann M., Scheper T., Schlüter M., Liese, A., 2012. Generation of Dean vortices and enhancement of oxygen transfer rates in membrane contactors for different hollow fiber geometries. Journal of membrane science, 423, 342-347.

Khosravi-Bizhaem H., Abbassi A., Ravan A. Z., 2019. Heat transfer enhancement and pressure drop by pulsating flow through helically coiled tube: An experimental study. Applied Thermal Engineering, 160, 114012.

Kurnia J. C., Chaedir B. A., Sasmito A. P., 2020. Laminar convective heat transfer in helical tube with twisted tape insert. International Journal of Heat and Mass Transfer, 150, 119309.

Liu S., Sakr M., 2013. A comprehensive review on passive heat transfer enhancements in pipe exchangers. Renewable and sustainable energy reviews, 19, 64-81.

Mishra P., Gupta S. N., 1979. Momentum transfer in curved pipes. 1. Newtonian fluids. Industrial & Engineering Chemistry Process Design and Development, 18(1), 130-137.

Przybył S., Pierański P., 2001. Helical close packings of ideal ropes. *The European Physical Journal E*, 4(4), 445-449.

Tohidi A., Hosseinalipour S. M., Shokrpour M., Mujumdar A. S., 2015. Heat transfer enhancement utilizing chaotic advection in coiled tube heat exchangers. Applied Thermal Engineering, 76, 185-195.

Wang G., Dbouk T., Wang D., Pei Y., Peng X., Yuan H., Xiang S., 2020. Experimental and numerical investigation on hydraulic and thermal performance in the tube-side of helically coiled-twisted trilobal tube heat exchanger. International Journal of Thermal Sciences, 153, 106328.

Webb R. L., Eckert E. R. G., 1972. Application of rough surfaces to heat exchanger design. International Journal of Heat and Mass Transfer, 15(9), 1647-1658.

Winzeler H. B., Belfort G., 1993. Enhanced performance for pressure-driven membrane processes: the argument for fluid instabilities. Journal of Membrane Science, 80(1), 35-47.

Wongcharee K., Eiamsa-Ard S., 2011. Friction and heat transfer characteristics of laminar swirl flow through the round tubes inserted with alternate clockwise and counter-clockwise twisted-tapes. International Communications in Heat and Mass Transfer, 38(3), 348-352.